

Elastic anomalies and orientational glass transition in $\text{Na}(\text{CN})_x\text{Cl}_{1-x}$ mixed crystals. A Brillouin spectroscopic study

R.J. Jiménez Riobóo^a, K.-P. Bohn, and J.K. Krüger

Fachrichtung Experimentalphysik 10.2, Universität des Saarlandes, Bau 38, Postfach 151150, 66041 Saarbrücken, Germany

Received 8 April 1999 and Received in final form 3 June 1999

Abstract. High performance Brillouin spectroscopy (BS) has been used to study the elastic properties (static and dynamic) of the orientational glassy state of $\text{Na}(\text{CN})_x\text{Cl}_{1-x}$ samples ($x < x_c \approx 0.65$). The temperature behaviour of the elastic properties reveals a more complex scenario for the orientational glass transition than generally believed. The shear elastic constant shows the well-known $c_{44}(T)$ anomaly, indicated by a minimum, found in other cyanide mixed crystals. The results obtained for the hypersonic attenuation are in clear contradiction with the dynamic character of the $c_{44}(T)$ -minimum. The temperature behaviour of the longitudinal elastic constant c_{11} of very dilute ($x < x_c$) $\text{Na}(\text{CN})_x\text{Cl}_{1-x}$ samples shows two striking features: i) Similar to the anomalous temperature behaviour of $c_{44}(T)$, lowering the temperature $c_{11}(T)$ first decreases, goes through a minimum and then rises again. The minimum takes place at a temperature above the temperature, T_{\min} , where $c_{44}(T)$ reaches its minimum value. ii) A kink-like anomaly of $c_{11}(T)$ is observed at lower temperatures. This second anomaly is similar to the classical one observed in canonical glasses at their glass transition temperature T_g .

PACS. 62.20.Dc Elasticity, elastic constants – 64.70.Pf Glass transitions – 78.35.+c Brillouin and Rayleigh scattering; other light scattering

1 Introduction

The concentration x strongly influences the structural phase transition behaviour of cyanide mixed crystals of the type $\text{M}(\text{CN})_x\text{Z}_{1-x}$ (where M and X denote alkali metals and Z represents halogenide ions) as compared to the pure alkali cyanides. For $\text{M}(\text{CN})_x\text{Z}_{1-x}$ crystals, the average cubic symmetry observed in the high temperature phase remains unchanged for all temperatures if the concentration is lower than a critical value x_c [1,2]. In this range ($x < x_c$) no structural phase transition is observed in the temperature dependence of different physical parameters. At a definite temperature, however, the system shows a minimum value of the shear elastic constant $c_{44}(T)$ that has been identified in the literature as a fingerprint of an orientational glass transition [1–18]. This behaviour totally differs from that of other orientational glasses which only show kink-like anomalies at the glass transition temperature [19], *i.e.* the same elastic phenomenology as in the case of canonical glasses [20]. The temperature where the $c_{44}(T)$ minimum takes place shows a frequency dependence, which suggests its dynamic character. At low frequencies this elastic behaviour presents spin-glass-like features [6,7]. As a representative of the $\text{M}(\text{CN})_x\text{Z}_{1-x}$

mixed crystals we chose the system $\text{Na}(\text{CN})_x\text{Cl}_{1-x}$. The temperature and concentration dependence of c_{44} , for $x > x_c$ ($x_c \approx 0.65$), was subject of a previous paper [8] and some previous results concerning the concentration range $x < x_c$ were also published [9].

The theoretical description of $c_{44}(x, T)$ has been the subject of numerous papers *e.g.* [7,10–12]. A consistent application of the model to the experimental data did not provide a satisfactory description of the temperature and concentration behaviour in the range $x > x_c$ [8]. The consistency of the theory requires that the concentration and temperature behaviour of c_{44} should be described with a unique set of parameters, independent of x and T in both concentration ranges $x > x_c$ and $x < x_c$.

In this paper we discuss high-resolution Brillouin spectroscopy (BS) results for $c_{44}(x, T)$ and $c_{11}(x, T)$ as well as for the hypersonic attenuations $\Gamma(x, T)$ for samples with $x < x_c$. In addition we performed ultrasonic (US) measurements on similar samples. A comparison reveals no systematic deviation between BS and US data. The behaviour of $c_{11}(T)$ at low temperatures (below liquid nitrogen temperature) provides a hint for the existence of a second elastic anomaly in these materials, which is very similar to the one found at the glass transition temperature in canonical glasses, as postulated in a previous paper [9] and observed in $\text{K}_x\text{Na}_{1-x}(\text{CN})$ [21].

^a Present address: LPMI, Faculté des Sciences, Université Nancy 1, B.P. 239 54506 Vandoeuvre-lès-Nancy, France
e-mail: Rafael.Jimenez@lpmi.uhp-nancy.fr

2 Experimental

The experiments were performed either on a 5-pass or on a 6-pass Fabry-Pérot interferometer (Sandercock) [22], using the 90A and 90R scattering geometries [23,24]. The light source was an Ar⁺ laser at a wavelength of $\lambda_0 = 514.5$ nm. A complete description of the set-up can be found in a previous paper [8].

The 90A scattering geometry has the advantage of not requiring the refractive index of the sample to evaluate the sound velocity; the corresponding acoustic wavelength is: $\Lambda^{90A} = \lambda_0/\sqrt{2}$. For the 90R scattering geometry the acoustic wave length Λ^{90R} depends on the refractive index n of the sample at the frequency of the laser light: $\Lambda^{90R} = \lambda_0/\sqrt{4n^2 - 2}$. Combining both scattering geometries for hypersound propagation in equivalent symmetry directions, one disposes of a very sensitive probe to detect dispersion processes (D^{90R} -function) [23,24]

$$D^{90R} = \left\{ \frac{1}{2} \left[\left(\frac{f^{90R}}{f^{90A}} \right)^2 + 1 \right] \right\}. \quad (1)$$

In the absence of hypersonic dispersion and for optically isotropic samples, the D^{90R} -function coincides with the refractive index n .

For the 90A scattering geometry the sound velocity is given by:

$$v(T) = \Lambda^{90A} f^{90A}(T), \quad (2)$$

where f stands for the frequency of the Brillouin shift. The acoustic wavelength in the case of the 90A scattering geometry is $\Lambda^{90A} = 363.8$ nm. The corresponding elastic constant is then:

$$c(T) = \rho(T)v^2(T), \quad (3)$$

where ρ is the mass density. The temperature dependence of the density is not known. Therefore, we assume the room temperature value to be valid at all T . This implies a T -dependent error in the evaluation of the elastic constant that is less than 1% over the whole temperature range [13]. If the phonon wave vector \mathbf{q} ($|\mathbf{q}| = 2\pi/\Lambda$) can be oriented parallel to a (100) direction of the cubic crystal, the elastic constant (3) corresponds to either $c_{11}(T)$ or $c_{44}(T)$ depending on the polarisation state of the scattered light.

The Pulse-Echo ultrasonic measurements were performed with a Matec Instruments Systems, model 6600. We used transducers of Parametrics (V156) at a frequency of 5 MHz.

The samples were cleaved pieces of Czochralski grown crystals. Dr. J. Albers and Dr. A. Klöpperpieper of the University of Saarland kindly provided these crystals. The cleaved samples showed a good optical quality and were used without further preparation for T -dependent measurements. The cleavage planes and corresponding edges provided a very accurate reference to orient the sample.

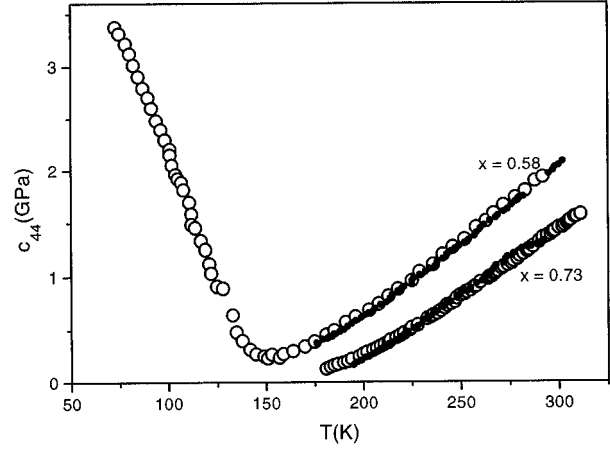


Fig. 1. Comparison of the temperature behaviour of the c_{44} data obtained by US (●) and BS (○) for $\text{Na}(\text{CN})_x\text{Cl}_{1-x}$ samples with $x = 0.73$ and $x = 0.58$.

3 Results and discussion

It is well-known that Czochralski grown $\text{Na}(\text{CN})_x\text{Cl}_{1-x}$ mixed crystals exhibit concentration gradients along the draw axis as well as perpendicular to it, in both concentration ranges ($x > x_c$ and $x < x_c$) [8,9]. The high resolution BS obtains information from a very small scattering volume ($\sim 10^{-7}$ cm³) which can be considered to be homogeneous. Therefore, existing concentration gradients do not affect the results. The influence of the gradients on experimental results obtained by other techniques using much larger information volumes (*i.e.* calorimetric measurements) [8] is difficult to answer.

In order to investigate possible systematic deviations in the values of the elastic constants obtained by different experimental techniques we took two samples of concentrations $x = 0.73$ ($x > x_c$) and $x = 0.58$ ($x < x_c$) and performed temperature dependent measurements of c_{44} with both ultrasonic (5 MHz) and Brillouin spectroscopy. In the case of pure NaCN a deviation of about +8% had been observed, the ultrasonic data being lower than the Brillouin ones [8]. This difference was interpreted as resulting from the influence of mosaic structures in the NaCN samples. The results on the mixed crystals are displayed in Figure 1. One observes an excellent agreement between the experimental data obtained with both techniques. The loss of ultrasonic signal at temperatures below 177 K for $x = 0.58$ is not due to a structural phase transition; it indicates the existence of a dispersion mechanism very efficient at ultrasonic frequencies but not at hypersonic ones. The same temperature dependent ultrasonic behaviour of the shear elastic constant was also observed, for instance, in $\text{Rb}(\text{CN})_x\text{Br}_{1-x}$ mixed crystals [15]. However, in BS investigations the $\text{Na}(\text{CN})_{0.58}\text{Cl}_{0.42}$ sample showed a clear lack of transparency around T_{\min} . This effect must be due to the existence of regions (clusters) which cause additional light scattering. These clusters could define zones of unchanged cubic symmetry but different refractive index.

A slight discrepancy in the slope of the $x = 0.73$ sample between the ultrasonic and Brillouin data is also

observed; this effect is believed to be due to mechanical constraints caused by the different expansion coefficients in the sample-bond and bond-transducer interfaces.

We investigated the T -dependence of c_{44} for the concentrations $x = 0.58$, $x = 0.30$ and $x = 0.20$ and of c_{11} for the concentrations $x = 0.12$ and $x = 0.22$. These concentrations belong to the range $x < x_c$ where glass transition behaviour is expected. First we discuss the results obtained for $c_{44}(T)$, shown in Figures 2a, 2b and 2c and in Table 1, as well as the T -dependence of the corresponding hypersonic attenuation.

As in the case of the critical concentration $x_c \approx 0.65$ [8,9], on lowering the temperature c_{44} decreases, goes through a minimum at T_{\min} and increases again. This increase is steeper than the decrease observed at higher temperatures. The value of T_{\min} changes with x , and it decreases at lower concentration. This temperature behaviour has been interpreted to correspond to the existence of an orientational glass transition [1–18] that must be understood in terms of a spin-glass-like transition. Indeed, the low frequency inverse elastic susceptibility (under field cooling and zero field cooling conditions) and the low frequency non-linear elastic susceptibility show very similar behaviours to those of real spin glasses [6,14].

In this context, theoretical approaches were developed to describe the x and T dependencies of the elastic shear mode [7,10–12]. The basic assumptions of these models can be summarised as follows: i) There exists a bilinear coupling between rotations of the CN^- ions and the lattice deformations (translation-rotation coupling). ii) There are random deformation fields, owing to the substitutional disorder, that depend on the concentration. iii) The bilinear coupling affects almost exclusively the shear elastic mode.

The main result of these models is summarised by the following expression:

$$c_{44}(T) = c_{44}^0 \frac{T - T_{01}(1 - q_{\text{EA}})}{T - T_{02}(1 - q_{\text{EA}})}, \quad (4)$$

where q_{EA} represents an Edwards-Anderson-like order parameter [7,12], c_{44}^0 stands for the background elasticity and T_{01} , T_{02} are concentration-dependent parameters. The determination of q_{EA} is a difficult task but an analytical approximation was given by the microscopical model developed by Michel [10,11]. The resulting T and x dependence of c_{44} can be written as:

$$c_{44}(T) = c_{44}^0 - \frac{Bx \left(1 - x(1-x) \left(\frac{T_2}{T}\right)^2\right)}{T + T_0x \left(1 - x(1-x) \left(\frac{T_2}{T}\right)^2\right)}. \quad (5)$$

Following the definitions of Michel, B represents the strength of the bilinear coupling, T_0 is a combination of the self-interaction of CN^- ions and the direct interaction between neighbouring CN^- - CN^- ions, T_2^2 gives the intensity of the random deformation fields due to the substitution of CN^- ions by halogenide ions, and c_{44}^0 is the background elasticity. In a first approximation, these parameters should be independent of the concentration, but

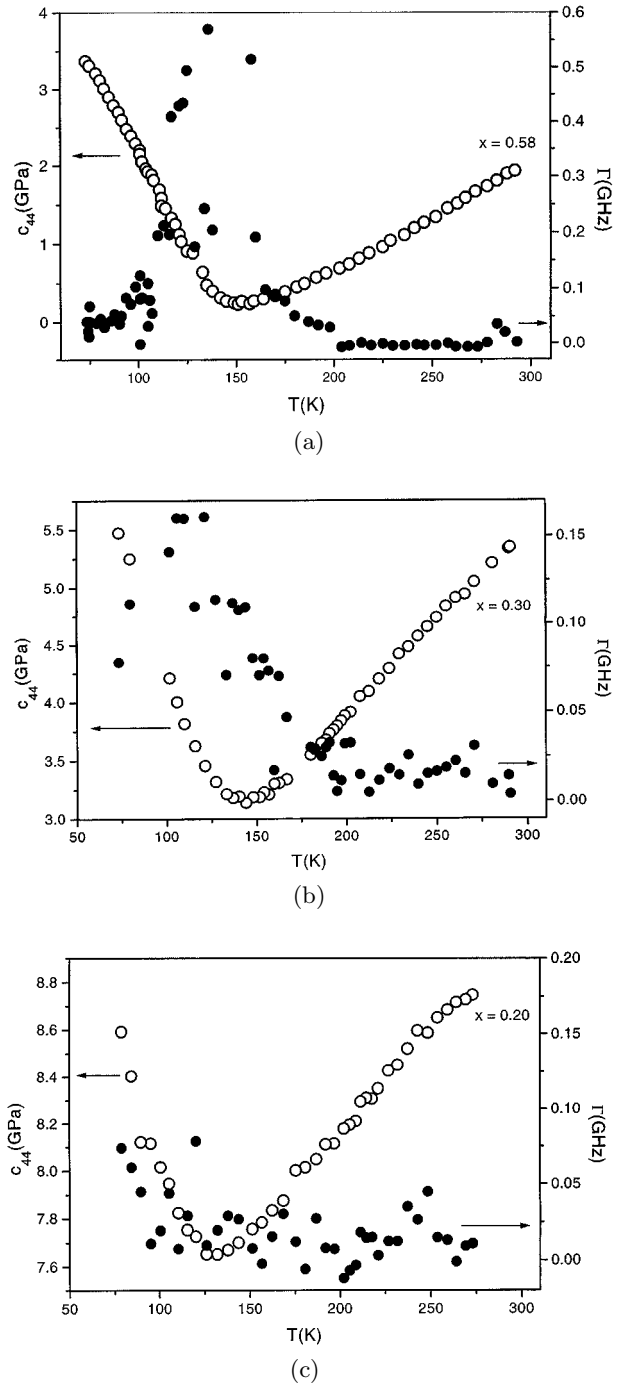


Fig. 2. Anomalous temperature behaviour of c_{44} (o) and corresponding attenuation Γ (●) for different $\text{Na}(\text{CN})_x\text{Cl}_{1-x}$ samples as obtained by BS with 90A scattering geometry. (a) $x = 0.58$, (b) $x = 0.30$ and (c) $x = 0.20$.

they are not universal constants valid for all mixed cyanide groups.

In a previous paper ($\text{Na}(\text{CN})_x\text{Cl}_{1-x}$, $x > x_c$) [8] we used this approximation and the results were unsatisfactory. Now, counting with experimental data in the range $x < x_c$, it is possible to implement the fit assuming a concentration dependence of B , T_0 , T_2 and keeping c_{44}^0

Table 1. Relevant experimental values for $\text{Na}(\text{CN})_x\text{Cl}_{1-x}$. x is the concentration, ρ the density, $c_{44}(\text{Ta})$ and $c_{11}(\text{Ta})$ the room temperature value of the shear and of the longitudinal elastic constants, Δc_{44} and Δc_{11} the increment between T_f and room temperature, T_f the temperature of the minimum (by this temperature the minimum of $c_{44}(T)$ or $c_{11}(T)$ takes place), T_m the temperature of the maximum (by this temperature the hypersonic attenuation maximum takes place, different for each elastic constant) and f_m the corresponding Brillouin frequency at T_m .

x	ρ (kg/m^3)	c_{44} (Ta) (GPa)	Δc_{44} (GPa)	T_f (K)	T_m (K)	f_m (GHz)
0.65	1794.38	1.673	1.595 (90A)	155	147.5	0.8233
	[8]					
0.58	1833.82	1.913	1.673 (90A)	152	140	1.203
0.30	1990.56	5.357	2.201 (90A)	146	107.2	3.878
			(90R)	154	122.3	7.2125
0.2	2046.62	8.867	1.216 (90A)	133	—	—
		$c_{11}(\text{Ta})$ (GPa)	Δc_{11} (GPa)			
0.22	2035.41	38.71	5.87 (90A)	135	104.4	11.6
			(90R)	149	133.4	22.15
0.12	2088.66	42.64	5.35 (90A)	123	88.8	12.35
			(90R)	135	95.5	24.53

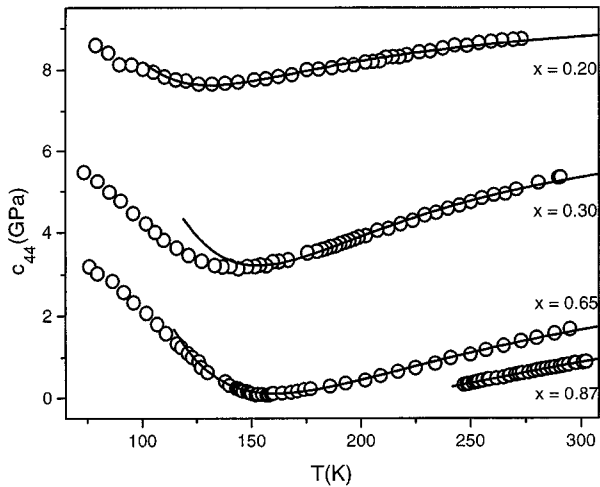


Fig. 3. $\text{Na}(\text{CN})_x\text{Cl}_{1-x}$. Experimental data and theoretical curves of c_{44} (according to (5)) assuming B , T_0 and T_2 concentration dependent. Further information see text.

as a constant, different for each concentration. The adjusted temperature ranges (in Kelvin) were: for $x = 0.87$, $240 < T < 310$; for $x = 0.65$, $155 < T < 300$; for $x = 0.30$, $145 < T < 300$ and for $x = 0.20$, $105 < T < 300$ (the 0.87 and 0.65 data stem from [8]). Figure 3 shows the simultaneous fits to the experimental data and Table 2 lists the obtained fitted values. T_2 is almost concentration independent for $x < x_c$, but shows a big change for $x > x_c$. All values were obtained by a simultaneous fit of all experiments.

The constancy of T_2 is clearly supported by the theory. Indeed, for $x > x_c$, it is possible to calculate a theoretical

Table 2. $\text{Na}(\text{CN})_x\text{Cl}_{1-x}$. Fit parameters obtained assuming a concentration dependence in B , T_0 , and T_2^2 (see (5)). c_{44}^0 was kept fixed during the fit procedure.

x	c_{44}^0 (GPa)	B (GPaK)	T_0 (K)	T_2^2 (K^2)
0.20	9.7	974.39	-512.89	35736.55
0.30	7.5	1432.28	-430.38	37174.27
0.65	4.40	1073.99	-131.68	38985.00
0.87	3.23	508.94	-188.78	120092.07

T_2 from x and T_{\min} [10–12]:

$$T_2^2 = \frac{T_{\min}^2}{3x(1-x)}. \quad (6)$$

The value we calculate from (6) for the different concentrations is $T_2^2 = 34560 \text{ K}^2$ that is very similar to the mean value obtained from the fit (see Tab. 2). This supports the view of theoretical models that the random fields play an important role in the transition behaviour. However, it also shows a limitation of the theory, which is not able to give a consistent picture of the random fields in both concentration ranges (above and below x_c).

T_2 is related to the intensity of the random deformation fields. Following Michel [10,11] $T_2 = h\xi^{1/2}$ where ξ is almost constant, $\xi \approx 0.07$. For the values of T_2 shown in Table 2 we obtain $h[\text{Cl}-\text{CN}] = 729 \text{ K}$. Brillouin measurements on $\text{K}(\text{CN})_x\text{Cl}_{1-x}$ [16] yield a lower value of $h(h[\text{Cl}-\text{CN}] = 450 \text{ K})$ [17]. This difference agrees with the fact that for the same concentrations ($x < x_c$) T_{\min} in $\text{K}(\text{CN})_x\text{Cl}_{1-x}$ lies lower than in $\text{Na}(\text{CN})_x\text{Cl}_{1-x}$ mixed crystals. This indicates that the difference in ionic radius of the alkali metal clearly influences the elastic behaviour. It is important to remember that the model is not valid for the temperature range of the $c_{44}(T)$ minimum as well as for $T < T_{\min}$.

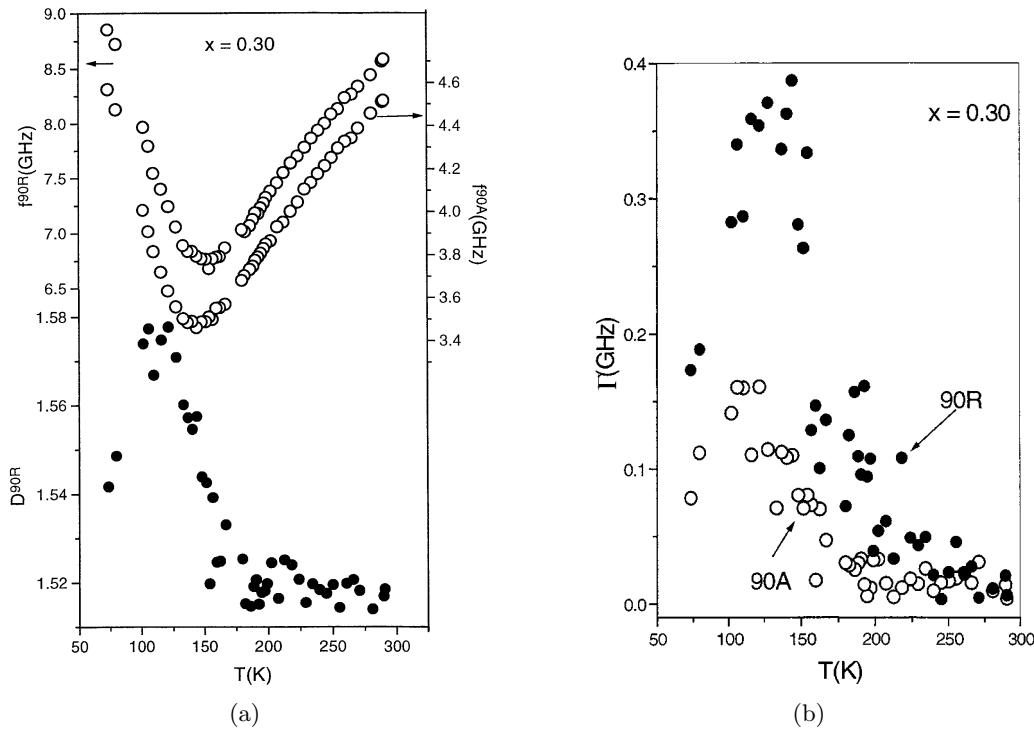


Fig. 4. (a) Temperature dependent $D^{90R}(T)$ -function and corresponding 90A and 90R Brillouin frequencies for the shear mode of $\text{Na}(\text{CN})_{0.30}\text{Cl}_{0.70}$. (b) Corresponding hypersonic attenuation for the 90A (o) and 90R (•) scattering geometries.

Besides the $c_{44}(T)$ -minimum an anomaly in form of a peak is observed in the hypersonic attenuation, Γ , (see Fig. 2). The maximum occurs at a temperature T_{max} that shifts to lower values with decreasing concentration [8, 9]. For the sample with $x = 0.20$ there is no attenuation anomaly detected in the temperature range studied.

The attenuation anomaly has usually been assumed to be intimately related to the existence of the $c_{44}(T)$ -minimum [2]. The theoretical model [11] took into account the existence of a relaxation frequency and the agreement between the theoretical model and the experimental attenuation was fair [18]. However, under this assumption, it has not been possible to account for the experimental temperature behaviour of c_{44} .

In order to get more insight into the nature of the hypersonic maximum we performed a simultaneous measurement of the Brillouin frequency shift using two different scattering geometries (90A and 90R) that provide symmetry equivalent phonon wave vectors of different length. The definition of the D^{90R} -function is given in equation (1). In the absence of acoustic dispersion, this function gives the temperature dependent refractive index of the sample. The investigated sample had a concentration $x = 0.30$. Figure 4a pictures the temperature dependence of the Brillouin frequency shift for both scattering geometries together with the resulting $D^{90R}(T)$ (the corresponding attenuation data are shown in Fig. 4b). If we assume the temperature dependence of the refractive index to be a smooth function of temperature, in the absence of acoustic dispersion $D^{90R}(T)$ should coincide with $n_{514.5}(T)$ (514.5 indicates the laser wave length

in nm). As expected, at room temperature the value of $D^{90R}(T)$ coincides with the value of the refractive index $n_{514.5}(T)$ ($n_D^{\text{R.T.}} = 1.5165$ obtained considering a linear concentration dependence between the values of NaCl and NaCN). At lower temperatures the $D^{90R}(T)$ -function shows an anomaly with a peak-like maximum, deviating thus from the smooth temperature dependence expected for $n_{514.5}(T)$. At still lower temperatures $D^{90R}(T)$ tends to meet $n_{514.5}(T)$ again; it has been shown that such deviations can be ascribed to the existence of acoustic dispersion [24]. Therefore the observed hypersonic attenuation anomalies reflect the dynamic properties of the studied sample.

The concentration dependences of T_{min} and T_{max} are clearly different (see Fig. 2 and also Refs. [8, 9]). Moreover, for small concentrations (*i.e.* $x = 0.20$) there is no detectable anomaly in the hypersonic attenuation, at least in the temperature range which has been investigated. If one compares the temperature behaviour of c_{44} , obtained by ultrasonics and Brillouin spectroscopy (Fig. 1, $x = 0.58$), it is clear that down to 175 K (hypersonic attenuation begins to grow quickly, see Fig. 2a) both techniques reflect the same elastic behaviour. Regarding the temperature position of the hypersonic attenuation maximum, it is clear that the temperature dependence of c_{44} , for both experimental techniques, and $T \geq 175$ K, is found to be in the “fast motion” regime ($\omega\tau \ll 1$) and the elastic response is always relaxed. At temperatures around and below the hypersonic attenuation maximum the elastic behaviour reflects the cross-over from the relaxed to the clamped elastic response of the “slow motion” regime

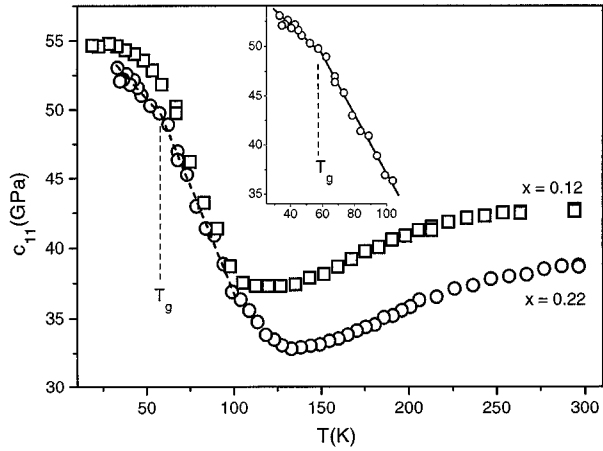


Fig. 5. Temperature dependence of the longitudinal acoustic mode $c_{11}(T)$ for a $\text{Na}(\text{CN})_{0.22}\text{Cl}_{0.78}$ sample (\circ) and a $\text{Na}(\text{CN})_{0.12}\text{Cl}_{0.88}$ sample (\square). $T_g = 60$ K is the temperature of the quasi-static glass transition.

($\omega\tau \gg 1$). As shown in Figures 2a, 2b and 2c and in Table 1, T_{\max} shifts to lower temperatures when the concentration decreases, and the temperature separation between T_{\min} and T_{\max} becomes larger the lower the concentration x . On the other hand, as far as the attenuation anomaly reflects acoustic dispersion, we expect the temperature position of the damping maximum for the US experiment to lie at temperatures clearly below T_{\max} .

In this context, the temperature behaviour of c_{44} , obtained for $x = 0.2$ (Fig. 2c) in the whole temperature range studied, represents the elastic response always in the “fast motion” regime ($\omega\tau \ll 1$). This behaviour is in clear contradiction with the assumption that the $c_{44}(T)$ -minimum is of dynamic origin and should show a frequency dependence (see for instance Ref. [2]). As proposed by the theoretical model, our results show that *the existence of a $c_{44}(T)$ -minimum is inherent to the translation-rotation coupling and does not need the presence of an attenuation maximum.*

The temperature dependence of the longitudinal elastic constant, $c_{11}(T)$, was investigated on two samples with concentrations $x = 0.22$ and $x = 0.12$. The first sample was investigated until 33 K and the second one until 18 K. The concentration values were obtained from the temperature and concentration dependence of the D^{90R} -function that gives the refractive index of the sample in the non dispersive temperature region. The temperature dependence of the corresponding longitudinal elastic constants c_{11} are shown in Figure 5 for both samples (the corresponding attenuation data are shown in Figs. 6a and 6b). It was surprising to find such a pronounced minimum in the longitudinal mode for these concentrations. It has usually been assumed that the main mechanism responsible for the phase transition behaviour in samples with $x > x_c$ and for the appearance of a minimum in the elastic constant, for $x < x_c$, is the bilinear coupling between lattice deformations and CN^- rotations, manifesting itself almost exclusively in the pure shear mode. A first theoret-

ical approach to describe the influence of the translation-rotation coupling on the longitudinal mode was proposed by Lynden-Bell and Michel [25] for $x = 1$. Within this frame, the effects to be observed in the longitudinal mode should be clearly weaker than those observed for the shear mode.

Contrary to the observations in the hypersonic attenuation of the shear mode for the $x = 0.20$ sample, the longitudinal mode shows a clear anomaly in the form of a peak in Γ for both samples. As can be seen in Figures 7a and 7b, the temperature dependent $D^{90R}(T)$ -function possesses a peak shaped anomaly for both concentrations. At room temperature this function coincides with the refractive index of the sample at the laser wavelength. This effect supports the existence of a dispersion that gives rise to an anomaly in the hypersonic attenuation. At 104.4 K we clearly observe an attenuation maximum in the longitudinal mode ($x = 0.22$ and 90A scattering geometry) and this maximum shifts to higher temperatures when using the 90R scattering geometry. It is important to notice that, contrary to the theoretical predictions, this damping maximum is much more pronounced than the attenuation maximum observed for the shear mode (compare for instance $x = 0.3$ and $x = 0.22$). It could be due to the existence of more than one dispersion mechanism in these systems.

These hypersonic dynamics are associated with at least one dispersion mechanism, clearly shown by the different D^{90R} -functions, that begins above T_{\min} and reaches its maximum just below T_{\min} for concentrations $x > 0.20$. The dispersion mechanisms discussed in the literature are related either to the dipolar relaxation or to the quadrupolar one. The latter has been related to the elastic behaviour. A first determination of the activation energy for the dipolar relaxation of a $\text{Na}(\text{CN})_x\text{Cl}_{1-x}$ sample was performed for $x = 0.43$ and is about $E = 358$ K [26]. It shows a tendency to diminish the lower the concentration x [26]. The activation energies related to the quadrupolar relaxation have been determined from the differences in the temperature position of the damping maximum obtained at low experimental frequencies (typically from 10 Hz to 1000 Hz) for the shear mode [14]. The estimated value for the activation energy of a sample with $x = 0.5$ is $E = 1265$ K [14].

Our BS data deliver information about the hypersonic attenuation (elastic damping) for 2 different wave vectors for each concentration x . In order to assess the type of activation process involved in the dynamic elastic behaviour (Arrhenius or Vogel-Fulcher-Tamman) and the corresponding activation energies, it is necessary to rely on more experimental points, covering a wide range of frequencies and that should be obtained with different experimental techniques. As the main experimental effort has been focused on the temperature behaviour of the elastic constants (almost exclusively on c_{44} , see for instance Ref. [2]) there is a lack of systematic study of the elastic damping that would allow to establish the type of activated process and related activation energy and to

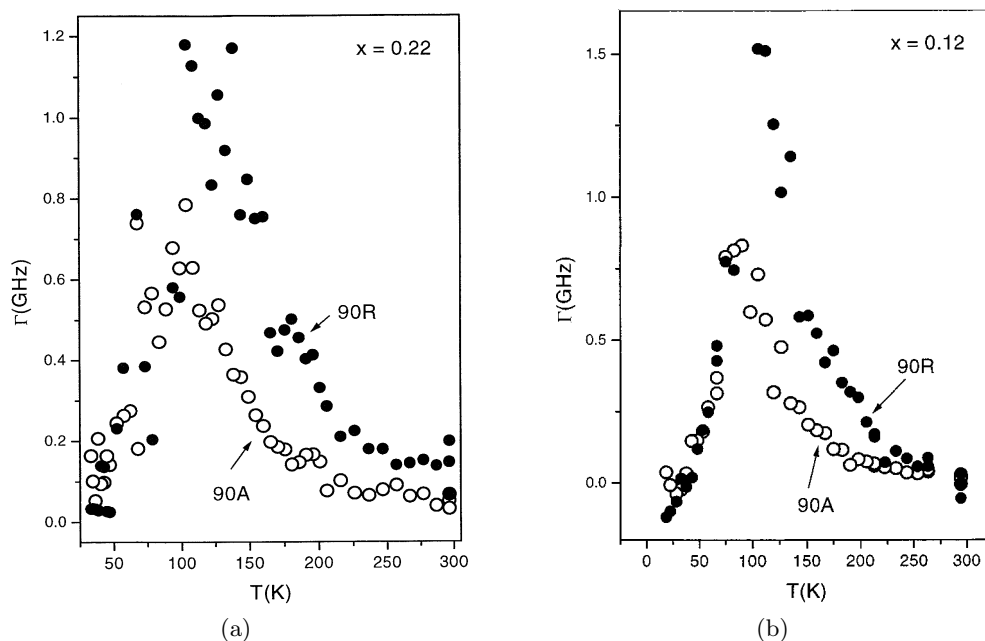


Fig. 6. Temperature dependence of the hypersonic attenuation for the 90A (o) and 90R (●) scattering geometries. (a) $\text{Na}(\text{CN})_{0.22}\text{Cl}_{0.78}$ sample, (b) $\text{Na}(\text{CN})_{0.12}\text{Cl}_{0.88}$ sample.

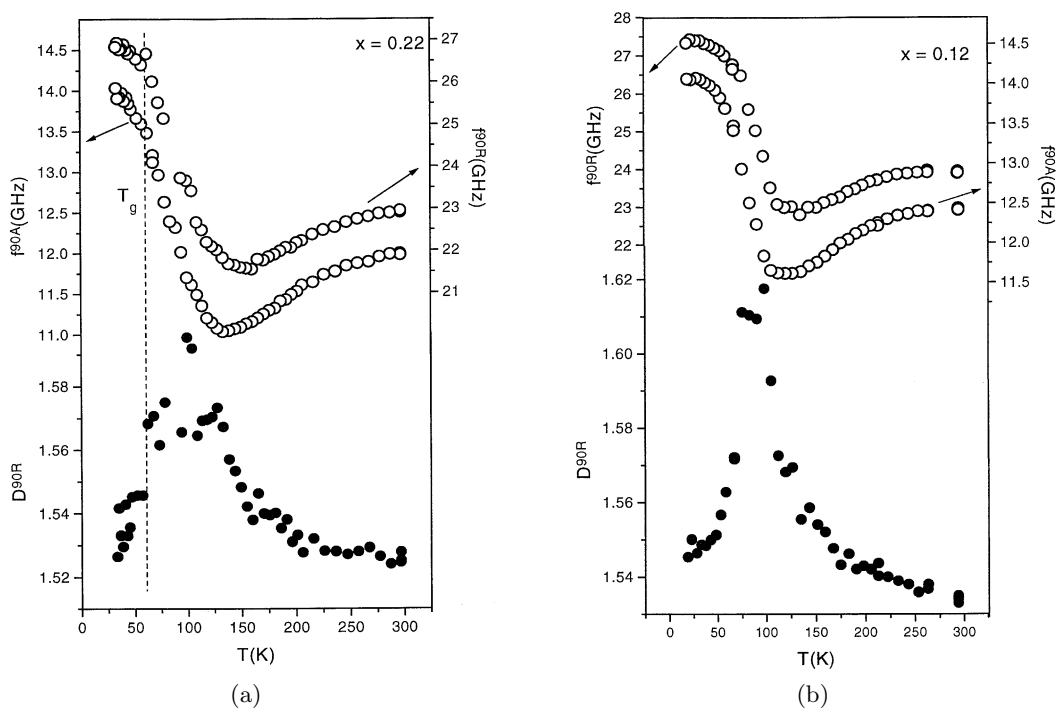


Fig. 7. Temperature dependence of the 90A and 90R Brillouin frequencies for c_{44} and corresponding D^{90R} -function for the $\text{Na}(\text{CN})_{0.22}\text{Cl}_{0.78}$ sample (a) and for the $\text{Na}(\text{CN})_{0.12}\text{Cl}_{0.88}$ sample (b). T_g is the quasi-static glass transition temperature.

determine the relation between the elastic damping of the shear elastic mode and that of the longitudinal mode (c_{11}).

As has been shown above, the existence of the $c_{44}(T)$ or $c_{11}(T)$ minima is independent of the appearance of a damping maximum (hypersonic attenuation). As in the classical glass formers, the hypersonic attenuation (especially that related to the longitudinal elastic mode) can be interpreted as the result of an α -relaxation process and the related temperature would be the dynamical glass transition temperature, being strongly frequency dependent. This dynamic would be the precursor of a glass transition to be found in the elastic constant at much lower temperatures. Phenomenologically, this glass transition would present the well-known characteristics of a classical glass transition in canonical glasses [27–29]. In a classical glass transition, the temperature dependent elastic constant is characterised by a kink-like anomaly at a defined temperature (quasi-static glass transition [20]), the slope being smaller in the low temperature branch.

This temperature behaviour of the elastic constants has been found in the case of the orientational glass 1,2-difluorotetrachloroethane and the $K_xNa_{1-x}(CN)$ mixed crystals [19,21]. In this way the $Na(CN)_xCl_{1-x}$ mixed crystals would share the same phenomenology with other orientational glasses.

Below the $c_{11}(T)$ -minimum temperature a huge increase of $c_{11}(T)$ is observed for both samples (Fig. 5). In the case of the $x = 0.22$ sample, there is a clear change of slope at 60 K. *This is resemblant of the typical fingerprint for a quasi-static glass transition.* The quasi-static character is corroborated by the fact that the kink-like anomaly is present and takes place at the same temperature in the 90A and 90R scattering geometries (see Fig. 7a). The temperature of the dynamical glass transition (T_m see Tab. 1) indicates that the classical glass transition for the $x = 0.12$ sample will take place at lower temperatures (at least 20 K below) than that found for the kink-like anomaly in the $x = 0.22$ sample. Indeed, for the $x = 0.12$ sample there is no kink-like anomaly at 60 K. The longitudinal elastic constant c_{11} begins to deviate from the linear behaviour at about 50 K and seems to stop abruptly around 30 K. This behaviour could be the indication of the expected classical glass transition in this sample.

These facts can be taken as evidence for the existence of a classical glass transition (regarding the elastic phenomenology) also in this kind of cyanide mixed crystals. This behaviour was also observed in $K_xNa_{1-x}(CN)$ mixed crystals [21]. The existence of two subsequent anomalies as characteristic for a glass transition in orientational glasses has been already shown in the case of RADP (see the review in Ref. [2]).

At this moment we have no explanation for the kind of relaxation process related to the α -relaxation. It could be related to the fact that the orientational frozen state might not correspond to a unique preferential orientation for the CN^- dumbbells, but to a coexistence of regions of different orientations that could be considered as orientational clusters. In the plastic phase of $K(CN)_xBr_{1-x}$ (a mixed crystal similar to $Na(CN)_xCl_{1-x}$) the CN^- dumb-

bells show a preferential orientation along the equivalent [111] cubic directions, but at low temperatures the orientation probability is higher along the equivalent [100] cubic directions [30]. The transition from one cluster to the neighbouring one defines a border region where the orientational state of the CN^- dumbbells is not well defined. These border regions will show their own dynamics that should freeze randomly at lower temperatures.

These orientational clusters could also be responsible for the existence of light efficient scattering regions (lack of transparency) observed about the $c_{44}(T)$ -minimum temperature.

4 Conclusions

The temperature dependence of the shear stiffness c_{44} in the case of NaCN as obtained by ultrasonic techniques, shows a systematic deviation from the Brillouin spectroscopic data. In order to investigate the existence of such incompatibility in the case of $Na(CN)_xCl_{1-x}$ mixed crystals, we performed $c_{44}(T)$ measurements using Brillouin spectroscopy as well as ultrasonic techniques. The results show an excellent agreement between the experimental data indicating that the mosaic structures (if present for $x < x_c$) responsible for such deviation in NaCN have no influence on the determination of the elastic properties of the mixed system *via* BS. The temperature dependence of the elastic shear modulus behaves anomalously as known from other cyanide mixed crystals for samples with concentrations $x < x_c$. The lack of ultrasonic signal, for instance in the $x = 0.58$ sample, is not accompanied by a lack of Brillouin signal but by a clear decrease in the transparency of the studied sample. This indicates the existence of light efficient structures (clusters) in a cubic symmetric crystal. These clusters produce a modulation of the refractive index resulting in a partial intransparency of the material. The influence of these clusters on the lack of signal in ultrasonic experiments cannot be evaluated due to the simultaneous existence of a big relaxation damping.

The theoretical analysis of the experimental data gives satisfactory results for concentrations $x < x_c$ above the minimum temperature and reveals the constraints of such models due, mainly, to the approximations used to describe the temperature and concentration dependence of the Edwards-Anderson-like order parameter. In order to obtain the best possible theoretical description of the experimental data, it is necessary to allow additional concentration dependences in the model parameters.

The hypersonic attenuation data and the temperature behaviour of the D^{90R} function relativize the dynamical character of $c_{44}(T)$. The concentration dependence of the hypersonic attenuation maximum is very different from that of the $c_{44}(T)$ -minimum and it is possible to find a minimum in $c_{44}(T)$ without a corresponding attenuation maximum. *The existence of a $c_{44}(T)$ -minimum is an inherent effect of the translation-rotation coupling and not the result of the existence of a maximum in the elastic damping and should not show a frequency dependence.*

Temperature dependent measurements of the longitudinal elastic constant, c_{11} , show a similar anomaly as in $c_{44}(T)$ (minimum value of $c_{11}(T)$) around the temperature T_{\min} even for samples with very low CN^- concentrations. The importance of this anomaly in the interpretation and understanding of the orientational glass transition behaviour has been, to our knowledge, neglected in the theoretical approaches to describe the anomalous elastic behaviour in the cyanide mixed crystals.

At lower temperatures $c_{11}(T)$ shows the typical kink-like anomaly found in order plastic crystals undergoing orientational glass transitions. The existence of different possible orientations of the CN^- dumbbells in the frozen state that could also be responsible for the lack of transparency around the c_{44} -minimum temperature and for the hypersonic attenuation maxima. The damping maximum would be the precursor of this second elastic anomaly with the typical elastic phenomenology found in other orientational glasses.

The kink-like anomaly takes place at $T_g = 60$ K for the $x = 0.22$ sample. Phenomenologically, this elastic behaviour is the same as the one found at T_g , the quasi-static glass transition temperature, for canonical and orientational glasses. A characteristic temperature of 30 K has been found for the $x = 0.12$ sample; the real glass transition temperature may lie higher but is masked by the expected anharmonic behaviour of $c_{11}(T)$ at low temperatures. The existence of two subsequent elastic anomalies was already observed in $\text{K}_x\text{Na}_{1-x}(\text{CN})$ mixed crystals, and seems to be inherent to this type of orientational glasses.

In the mixed crystals of the type $\text{Na}(\text{CN})_x\text{Cl}_{1-x}$ and $\text{K}_x\text{Na}_{1-x}(\text{CN})$, the glass transition behaviour is more complicated than generally believed. The elastic behaviour in the concentration range $x < x_c$ supports the existence of two elastic anomalies.

The elastic behaviour of the cyanide mixed crystals is much more in accordance with the one observed in other orientational glasses that show the typical kink-like anomaly in the elastic constants at the orientational glass transition than believed until now.

References

1. K. Knorr, Phys. Scripta **19**, 531 (1987).
2. U.T. Höchli, K. Knorr, A. Loidl, Adv. Phys. **39**, 405 (1990).
3. S.K. Satija, C.H. Wang, Solid St. Commun. **28**, 617 (1978).
4. S. Elschner, J. Petersson, J. Albers, J. K. Krüger, Ferroelectr. **78**, 43 (1988).
5. Z. Hu, D. Walton, J.J. Vanderwal, Phys. Rev. B **38**, 10830 (1988).
6. a) J. Hessinger, K. Knorr, Phys. Rev. Lett. **65**, 2674 (1990); b) J. Hessinger, K. Knorr, Ferroelectr. **127**, 29 (1992).
7. W. Wiotte, J. Petersson, R. Blinc, S. Elschner, Phys. Rev. B **43**, 12751 (1991).
8. J.K. Krüger, R. Jiménez, K.-P. Bohn, J. Petersson, J. Albers, A. Klöpperpieper, E. Sauerland, H.-E. Müser, Phys. Rev. B **42**, 8537 (1990).
9. R. Jiménez, K.-P. Bohn, J. K. Krüger, J. Petersson, Ferroelectr. **106**, 175 (1990).
10. K.H. Michel, Phys. Rev. B **35**, 1405 (1987).
11. K.H. Michel, Phys. Rev. B **35**, 1414 (1987).
12. J.O. Fossum, A. Wells, C.W. Garland, Phys. Rev. B **38**, 412 (1988).
13. A. Loidl, T. Schröder, R. Böhmer, K. Knorr, J.K. Kjems, R. Born, Phys. Rev. B **34**, 1238 (1986).
14. C. Kaiser, Ph.D. thesis, Saarbrücken, 1995.
15. C.W. Garland, J.O. Fossum, Z. Hu, A. Wells, Phys. Rev. B **41**, 12210 (1990).
16. C.H. Wang, S. Satija, F. Luty, Chem. Phys. Lett. **90**, 397 (1982).
17. J.O. Fossum, C.W. Garland, Phys. Rev. Lett. **60**, 592 (1988).
18. Z. Hu, D. Walton, J.J. Vanderwal, Phys. Rev. B **38**, 10830 (1988).
19. J.K. Krüger, J. Schreiber, R. Jiménez, K.-P. Bohn, F. Smutný, M. Kubát, J. Petzelt, J. Hrabovská-Bradshaw, S. Kamba, J.F. Legrand, J. Phys. Cond. Matter **6**, 6947 (1994).
20. J.K. Krüger, K.-P. Bohn, R. Jiménez, J. Schreiber, Colloid Polymer Sci. **274**, 490 (1996).
21. R. Jiménez, B. Jiménez, J.K. Krüger, J. Schreiber, F. Sayetat, F. Mauvy, Ferroelectr. **157**, 141 (1994).
22. J.R. Sandercock, *Light scattering in solids III*, Topics in Applied Physics **51** (Springer, Berlin, 1982), Chap. 6.
23. J.K. Krüger, L. Peetz, M. Pietralla, Polymer **19**, 1397 (1978).
24. J.K. Krüger, A. Marx, L. Peetz, H.-G. Unruh, Colloid Polymer. Sci. **264**, 403 (1986).
25. R.M. Lynden-Bell, K.H. Michel, Rev. Mod. Phys. **66**, 721 (1994).
26. R. Bastuck, Ph.D. thesis, Saarbrücken, 1992.
27. J.K. Krüger, Brillouin Spectroscopy and its application to Polymers in *Optical techniques to characterize polymer systems*, edited by A. Bäessler (Elsevier, Amsterdam, 1989).
28. M. Foulon, J.P. Amoureux, J.L. Sauvajol, J.P. Cavrot, M. Muller, J. Phys. C Solid State Phys. **17**, 4213 (1984).
29. M. Grimsdich, L.M. Torell, *Dynamics of disorder materials* (Springer, proceedings in Physics **37**, 196 (1989)).
30. A. Loidl, K. Knorr, J.M. Rowe, G.J. McIntyre, Phys. Rev. B **37**, 389 (1988).